Quantitative theory for the lateral momentum distribution after strong-field ionization

Ingo Dreissigacker*, Manfred Lein

Institut für Theoretische Physik and Centre for Quantum Engineering and Space-Time Research (QUEST),
Leibniz Universität Hannover, Appelstraße 2, D-30167 Hannover, Germany

Abstract

We investigate theoretical models for the lateral width of the electron momentum distribution after recollision-free strong-field ionization of atoms. We review the derivation of the tunneling formula and demonstrate that the pre-exponential factor in the saddle-point approximation cannot be neglected if quantitative results are desired. We calculate the widths for hydrogen as well as argon and neon atoms. We compare to results from the time-dependent Schrödinger equation, and to the experimental results from [Arissian et al., Phys. Rev. Lett. 105, 133002 (2010)].

Keywords: strong-field ionization, angular streaking, lateral momentum distribution, tunneling formula

The availability of light sources capable of producing ultra-short pulses in the femtosecond [1] and even the attosecond regime [2] has led to numerous new applications, such as generation of coherent soft x-rays [3], attosecond imaging of molecular electronic wave packets [4], real-time observation of atomic-scale electron dynamics [5, 6], and probing of molecular dynamics with subfemtosecond resolution [7]. In attosecond science [8], angular streaking with elliptically or circularly polarized pulses may become an important tool to measure the carrier-envelope-phase (CEP) of few-cycle laser pulses [9]. Angular streaking has already been used to put a small upper limit on the tunneling delay time [10, 11]. Furthermore, ionization of atoms by circularly polarized light has brought new insight into tunneling ionization via measurement of the lateral momentum distribution, *i.e.* the distribution in the direction perpendicular to the laser field [12]. While linear polarization leads to strong Coulomb effects in the lateral distributions [13, 14], for circular polarization, the width of the lateral distribution is approximately predicted by a simple tunneling formula [15, 16].

*Corresponding author
Email address: ingo.dreissigacker@itp.uni-hannover.de (Ingo Dreissigacker)

It can therefore be used to improve [17] measurements of peak intensities via momentum distributions [18]. It has been demonstrated theoretically that the lateral width corresponds to the instantaneous electric field at the moment of ionization, even at high field amplitudes for which substantial depletion takes place [19]. This enables precise measurements of the CEP or the peak field amplitudes, if the dependence of the width on the field is known accurately enough from theory. However, in the experiment by Arissian *et al.* [12], a difference of about 15% between the measured widths and the predictions of the tunneling formula has been found.

In this paper, we revisit the tunneling formula, and we find reasons for its deficiencies. We re-derive the expression with the correct prefactor by applying the saddle-point approximation to the strong field approximation (SFA). We demonstrate that it is actually capable of describing the lateral width very accurately. We use atomic units throughout this paper.

The previously used tunneling formula predicts - up to a non-constant prefactor - a simple Gaussian dependence of the momentum distribution $|M(\mathbf{k})|^2$ on the lateral momentum component $k_\perp$ [12, 15, 20],

$$|M(\mathbf{k})|^2 \propto P_{0\perp}(k_\perp)\, \exp\left(-k_\perp^2\, \frac{\sqrt{2\,I_p}}{E_0}\right). \tag{1}$$

The prefactor $P_{0\perp}(k_\perp)$ is the momentum distribution of the initial state, *i.e.* $P_{0\perp} = \int \mathrm{d}k_z\, |\tilde{\psi}_0(k_\perp, 0, k_z)|^2$ with $\tilde{\psi}_0(k_x, k_y, k_z)$ being the initial-state momentum-space wave function, assumed to be cylindrically symmetric [12, 20]. However, even with the non-adiabatic version of the tunneling formula [21], which replaces the Gaussian in Eq. (1) by an improved expression, Arissian *et al.* have found a difference of about 15% between the measured and the predicted widths of the lateral momentum distribution. In this work, we find that the inaccuracy originates mainly from the heuristic prefactor $P_{0\perp}(k_\perp)$, which does not arise rigorously from the derivation of the tunneling formula. We show results for hydrogen, argon, and neon atoms. We compare to the results obtained independently from time-dependent Schrödinger equation (TDSE) calculations in the case of hydrogen, and to the experimental results of Arissian *et al.* [12] in the case of argon and neon. For hydrogen, we additionally solve the SFA integral numerically in order to assess the error introduced by the saddle-point approximation. In all cases, we find that the saddle-point approximation with the correct prefactor predicts the lateral width more accurately than the simple tunneling formula.

In the SFA approach, the momentum distribution of an electron after strong-field ionization is the modulus squared of the SFA transition amplitude (Keldysh-Faisal-Reiss amplitude) [22–24], which reads

$$M(\mathbf{k}) = -i \int_{t_0}^{t_f} \mathrm{d}t\, \langle \mathbf{k} + \mathbf{A}(t) | \mathbf{r} \cdot \mathbf{E}(t) | \psi_0 \rangle\, e^{iS(\mathbf{k},t)} \tag{2}$$

in the length gauge. Here, $\mathbf{E}(t)$ is the electric field exerted to the atom by the laser pulse, $\mathbf{A}(t) = -\int^t \mathrm{d}t'\, \mathbf{E}(t')$, and $S(\mathbf{k}, t) = 1/2 \int_{t_0}^t \mathrm{d}t'\, (\mathbf{k} + \mathbf{A}(t'))^2 +$

$I_p\,(t-t_0)$ is the action. The interaction of the atom with the laser field takes place between the times t_0 and t_f. The final velocity of an outgoing electron is given by $\mathbf{v}_f = \mathbf{k} + \mathbf{A}(t_f)$. The matrix element $\mathcal{D}(\mathbf{k},t) = \langle \mathbf{k} + \mathbf{A}(t)|\mathbf{r}\cdot\mathbf{E}(t)|\psi_0\rangle$ describes the transition from an initial bound state ψ_0 to a plane-wave state with kinetic momentum $\mathbf{k} + \mathbf{A}(t)$. After this transition, the interaction of the electron with the ion is neglected. It can be calculated easily if the bound-state momentum-space wave function $\tilde{\psi}_0(\mathbf{p}) = (2\pi)^{-3/2}\int \mathrm{d}^3r\,\psi_0(\mathbf{r})\,e^{-i\mathbf{p}\cdot\mathbf{r}}$ is known:

$$\langle \mathbf{k} + \mathbf{A}(t)|\mathbf{r}\cdot\mathbf{E}(t)|\psi_0\rangle = i\,\mathbf{E}\cdot\nabla_{\mathbf{p}}\tilde{\psi}_0(\mathbf{p})\Big|_{\mathbf{p}=\mathbf{k}+\mathbf{A}(t)}. \tag{3}$$

For hydrogen-like atoms with nuclear charge Z, the momentum-space wave functions are known analytically for any choice of quantum numbers n, l, m [25]:

$$\begin{aligned}\tilde{\psi}_{nlm}(p,\theta,\phi) = &\left\{\frac{1}{(2\pi)^{1/2}}e^{im\phi}\right\}\left\{\left(\frac{(2l+1)(l-m)!}{2(l+m)!}\right)^{1/2}P_l^m(\cos\theta)\right\}\\ &\times\left\{\frac{2^{2l+5/2}l!}{\pi^{1/2}\,\gamma^{3/2}}\left(\frac{n(n-l-1)!}{(n+l)!}\right)^{1/2}\frac{\zeta^l}{(\zeta^2+1)^{l+2}}\,C_{n-l-1}^{l+1}\left(\frac{\zeta^2-1}{\zeta^2+1}\right)\right\},\end{aligned} \tag{4}$$

where $\zeta = p/\gamma$, $\gamma = Z/n$, P_l^m is the associated Legendre function, and C_{n-l-1}^{l+1} is the Gegenbauer polynomial.

Since the exponential in Eq. (2) oscillates rapidly with time, use of the saddle-point approximation is justified. Here, we restrict ourselves to a linearly polarized half-cycle laser pulse $\mathbf{E}(t) = E_0\,\mathbf{e}_z\,\sin(\omega t)$ with $\mathbf{A}(t) = \mathbf{e}_z\,E_0/\omega\,\cos(\omega t)$ in order to avoid interference effects between different saddle points. Agreement of the width from a linearly polarized half-cycle pulse with that from a circularly polarized pulse has been demonstrated in TDSE calculations [19]. The saddle-point condition reads

$$\dot{S}(\mathbf{k},t_s) = 0, \tag{5}$$

which, with the definition of $S(\mathbf{k},t)$, immediately implies

$$(\mathbf{k} + \mathbf{A}(t_s))^2 = -2\,I_p, \tag{6}$$

and

$$t_s = \frac{1}{\omega}\arccos\left[-\frac{\omega}{E_0}\,\left(k_z + i\,\sqrt{k_x^2 + k_y^2 + 2\,I_p}\right)\right]. \tag{7}$$

If we compare Eq. (6) to the hydrogen momentum-space wave functions, we observe that all matrix elements for hydrogen have a pole at the saddle point [25, 26]. With a generalized saddle-point formula, we can find the following approximation (for a derivation, see [26], Appendix B),

$$\begin{aligned}\int_{-\infty}^{\infty}\mathrm{d}t\,\mathcal{D}(\mathbf{k},t)\,e^{iS(\mathbf{k},t)} \approx i^q\,&\sqrt{\frac{2\,\pi}{-i\,\ddot{S}(\mathbf{k},t_s)}}\,\frac{\Gamma(q/2)}{2\,\Gamma(q)}\,\tilde{\mathcal{D}}(\mathbf{k},t_s)\\ &\times\left(-2\,i\,\ddot{S}(\mathbf{k},t_s)\right)^{q/2}\,e^{iS(\mathbf{k},t_s)},\end{aligned} \tag{8}$$

where q is the order of the pole, and $\tilde{\mathcal{D}}(\mathbf{k}, t_s) = \lim_{t\to t_s} \mathcal{D}(\mathbf{k}, t)(t - t_s)^q$. If we additionally change the integration interval in Eq. (2) to $(-\infty, \infty)$, Eq. (8) is an approximation to the integral in Eq. (2).

As a consistency check, we note that taking the adiabatic limit $\omega \to 0$ in the exponential, we obtain

$$|M(\mathbf{k})|^2 \approx |\mathcal{P}(\mathbf{k})|^2 \, \exp\left(-\frac{2\sqrt{k_x^2 + k_y^2 + 2\,I_p}^{\,3}}{3\,E_0}\right), \tag{9}$$

where Taylor expansion of the exponent with respect to $k_\perp$ yields the same Gaussian dependence as in the tunneling formula, Eq. (1) [21]. However, the prefactor $|\mathcal{P}(\mathbf{k})|^2$ that stems from Eq. (8) is not simply the initial-state momentum-distribution. Instead, the correct prefactor is

$$|\mathcal{P}(\mathbf{k})|^2 = 4\,\pi \left(\frac{\Gamma(q/2)}{2\,\Gamma(q)}\right)^2 \left|2\,\ddot{S}(\mathbf{k}, t_s)\right|^{q-1} |\tilde{\mathcal{D}}(\mathbf{k}, t_s)|^2, \tag{10}$$

which leads (without taking the adiabatic limit) to a quantitave tunneling formula (QTF),

$$\begin{aligned} |M(\mathbf{k})|^2 = 4\,\pi \left(\frac{\Gamma(q/2)}{2\,\Gamma(q)}\right)^2 & |2\,(\mathbf{k} + \mathbf{A}(t_s)) \cdot \mathbf{E}(t_s)|^{q-1} \\ & \times |\tilde{\mathcal{D}}(\mathbf{k}, t_s)|^2 \, |\exp\left(i\,S(\mathbf{k}, t_s)\right)|^2 . \end{aligned} \tag{11}$$

As the first application of our model, we consider a linearly polarized half-cycle laser pulse of 800 nm wavelength acting on the hydrogen 1s ground state. The resulting momentum distributions are centered at $\mathbf{v}_f = -\mathbf{e}_z\, E_0/\omega$ corresponding to $\mathbf{k} = 0$ since $\mathbf{A}(t_f) = -\mathbf{e}_z\, E_0/\omega$. We fit Gaussians $\exp(-k_\perp^2/\sigma^2)$ to the lateral momentum distributions

$$L_{k_z}(k_\perp) = \int \mathrm{d}k'_\perp \, |M(k_\perp, k'_\perp, k_z)|^2 \tag{12}$$

at $k_z = 0$ in order to obtain the respective width σ. Note that $v_{f,\,z} = -E_0/\omega$ corresponds to ionization at the maximum of the electric field and thus maximizes approximately the width [19]. We calculate the width using the QTF, Eq. (11), and by direct numerical integration of the SFA integral, Eq. (2). Additionally, we solve the TDSE

$$i\,\partial_t \psi(\mathbf{r}, t) = \left(-\frac{\nabla^2}{2} + \mathbf{r} \cdot \mathbf{E}(t) - \frac{1}{r}\right) \psi(\mathbf{r}, t) \tag{13}$$

on a large grid in cylindrical coordinates to have an exact reference. We use the split-operator method to propagate the wave function with a time step of 0.0125 a.u. on a grid comprising 1536 points in lateral direction and 6144 points in field direction, covering 225×900 a.u. in total. We continue to propagate

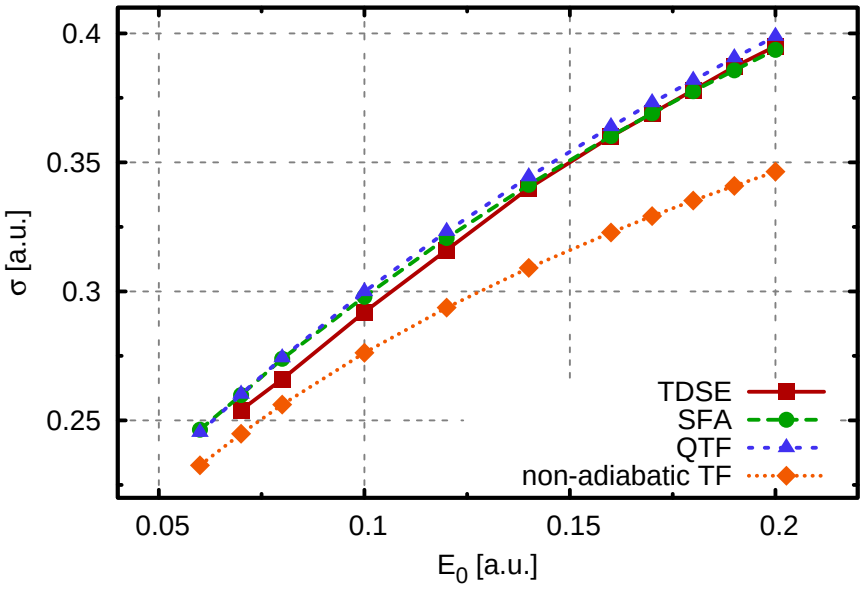

Figure 1: Lateral width σ of the momentum distribution after strong-field ionization of the hydrogen atom by an 800 nm half-cycle pulse at different field amplitudes E_0. Shown are results from the TDSE (red squares), direct computation of the SFA integral, Eq. (2), (green circles), the quantitative tunneling formula (QTF), Eq. (11), (blue triangles), and the non-adiabatic tunneling formula (TF), Eq. (14), (orange diamonds).

the wave function $\psi(\mathbf{r}, t)$ after the end of the half-cycle pulse until the wave packet is sufficiently far from the ion to obtain the final momentum-space wave function $\tilde{\psi}(\mathbf{p})$ by Fourier transformation.

In Fig. 1, the resulting lateral widths σ are shown for the hydrogen atom over a large range of field amplitudes E_0. We observe that the saddle-point approximation is a very accurate approximation to the SFA integral, which in turn is an accurate approximation to the exact solution of the problem. Shown are also results of the non-adiabatic tunneling formula

$$|M(\mathbf{k})|^2 \propto P_{0\perp}(k_\perp)\ |\exp\left(i\,S(\mathbf{k}, t_s)\right)|^2\,, \tag{14}$$

where the exponential is the full non-adiabatic expression from the saddle-point SFA, but the prefactor is kept as in the simple tunneling formula. The exponential is the same as the one derived in [21]. The widths obtained from Eq. (14) deviate significantly from those of the TDSE. The simple adiabatic tunneling formula yields even smaller widths and is therefore not shown. We emphasize that the large difference between the non-adiabatic tunneling formula, Eq. (14), and the QTF, Eq. (11), is solely due to the prefactor, since the exponential part is treated equally in both cases.

Inspired by the great improvement in accuracy for the hydrogen atom, we

apply our approach also to the argon and the neon atom. These atoms were used in the experiment by Arissian *et al.* [12]. However, the lack of knowledge about the matrix element $\mathcal{D}(\mathbf{k}, t)$ requires additional approximations in these cases. An approximation for the momentum-space wave function $\tilde{\psi}_0$ – and thus via Eq. (3) for the matrix element – can be found by treating all electron orbitals as hydrogen-like [25] with effective nuclear charges $Z_{\mathrm{eff},nl}$ for each orbital. These are found by a self-consistent optimization scheme for the energy [27]. As in [12], we use a value of $Z_{\mathrm{eff},31} = 6.764$ for the argon 3p orbital, and a value of $Z_{\mathrm{eff},21} = 5.758$ for the neon 2p orbital [27]. For simplicity, we drop the indices nl of Z_{eff} in the following. To assess the approximation for the bound state, we compare the momentum-space distributions calculated in this way to those obtained by solving the static Schrödinger equation for a single active electron in a suitable effective potential. The potentials for argon and neon are taken from [28, 29] and [30], respectively. The momentum distributions for $m = 0$, integrated along k_z are shown in Fig. 2(a) for the argon atom and 2(c) for the neon atom. Additionally, the longitudinal distributions $P_{0\|}(k_z) = \int \mathrm{d}k_x \mathrm{d}k_y \, |\tilde{\psi}_0(k_x, k_y, k_z)|^2$ are shown in Figs. 2(b) and 2(d) for argon and neon, respectively. We observe that for argon, the simple hydrogen-like momentum distribution is (at least for small momenta) very close to the more accurate single-active-electron approximation. Since the SFA integrand oscillates strongly for large momenta, we expect small momenta in the matrix element to have the greatest impact on the resulting SFA amplitude. Therefore, we expect reasonable results for argon using the hydrogen-like orbital. In case of the neon atom, however, the momentum distributions differ over the entire range of momenta. Since the hydrogen-like model provides only a rough approximation to the momentum distribution, we expect less accurate results for the lateral width in the neon case.

Use of the hydrogen-like orbitals has the advantage that the matrix element does not exhibit a pole at the saddle-point time t_s, since $I_p \neq Z_{\mathrm{eff}}/(2n^2)$. Therefore, we can use Eq. (11) with $q = 0$. For both argon and neon, we assume all ionization is from the outermost orbital with $m = 0$ because the orbital aligned with the field dominates in strong-field ionization.

For argon, the $3\mathrm{p}_z$ momentum-space wave function reads

$$\tilde{\psi}_{310}(p, \theta, \phi) = N \, p \, \cos\theta \, \frac{p^2 - Z_{\mathrm{eff}}^2/n^2}{(p^2 + Z_{\mathrm{eff}}^2/n^2)^4}, \tag{15}$$

with a normalization constant N. Inserting this into Eq. (11) with $q = 0$ and using Eq. (3), we calculate the momentum distribution. Again, we fit Gaussians $\exp(-k_\perp^2/\sigma^2)$ to the lateral distribution at $k_z = 0$ to obtain the lateral width σ. The results are shown in Fig. 3 in comparison to experimental values taken from [12] and to the adiabatic and non-adiabatic forms of the tunneling formula, Eqs. (1) and (14), respectively. We find that the results from the QTF are much more accurate than those from the other tunneling formulas. In fact, our curve lies entirely within the error bars of the measurement. This is a remarkable result given the simplicity of the applied approximations.

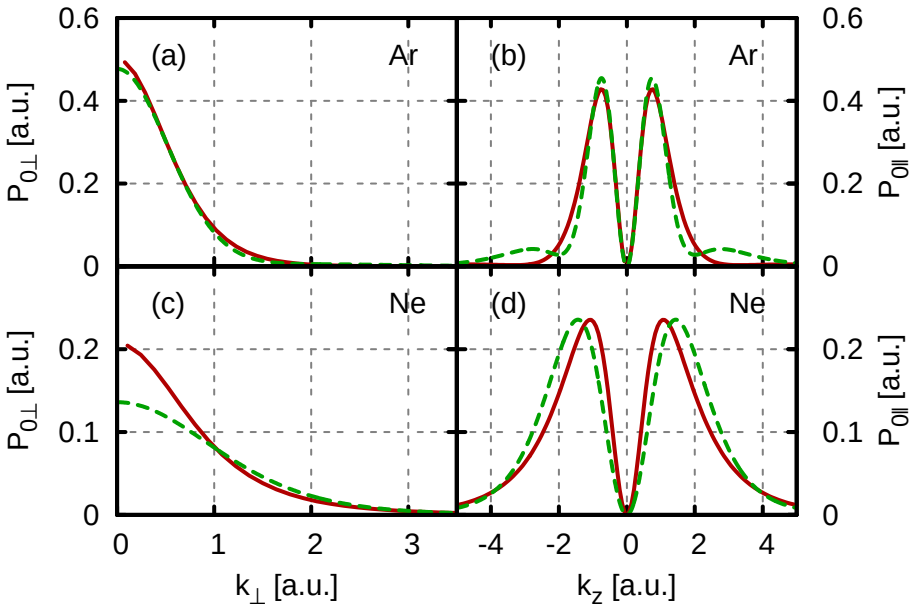

Figure 2: Valence-orbital momentum distributions of argon integrated along k_z (a) and $k_\perp$ (b), and neon, also integrated along k_z (c) and $k_\perp$ (d). The solid red curves show the momentum distributions from an effective single-active-electron potential [28, 30] the dashed green curves show the hydrogen-like $3p_z$ momentum distribution from Eq. (15) with $Z_{\text{eff}} = 6.76$ for argon ((a),(b)) and the hydrogen-like $2p_z$ momentum distribution from Eq. (16) with $Z_{\text{eff}} = 5.76$ for neon ((c),(d)).

For neon, the $2p_z$ momentum-space wave function reads

$$\tilde{\psi}_{210}(p,\theta,\phi) = N' \frac{p\,\cos\theta}{(p^2 + Z_{\text{eff}}^2/n^2)^3}, \tag{16}$$

with a normalization constant N'. We calculate the momentum distribution after ionization, applying the same procedure as for the argon atom. In Fig. 4, the results for neon are shown in comparison to the experimental results from [12] and the results of the adiabatic and non-adiabatic tunneling formulas, Eqs. (1) and (14), respectively. Again, the simple tunneling formulas yield too narrow distributions, both in the adiabatic and the non-adiabatic version. The QTF improves the predictions, but in contrast to the case of the argon atom, a significant difference to the measurement remains. This can well be due to the less accurate momentum distribution used in the calculation of the matrix element.

In conclusion, we have investigated the tunneling formula for the width of the lateral electron momentum distribution after strong-field ionization. We found that the pre-exponential factor is important if quantitatively reliable values are desired. Applying the saddle-point approximation to find the correct prefactor yields remarkably accurate results in the infrared regime. This will stimulate further research on measuring the lateral width as a diagnostic tool

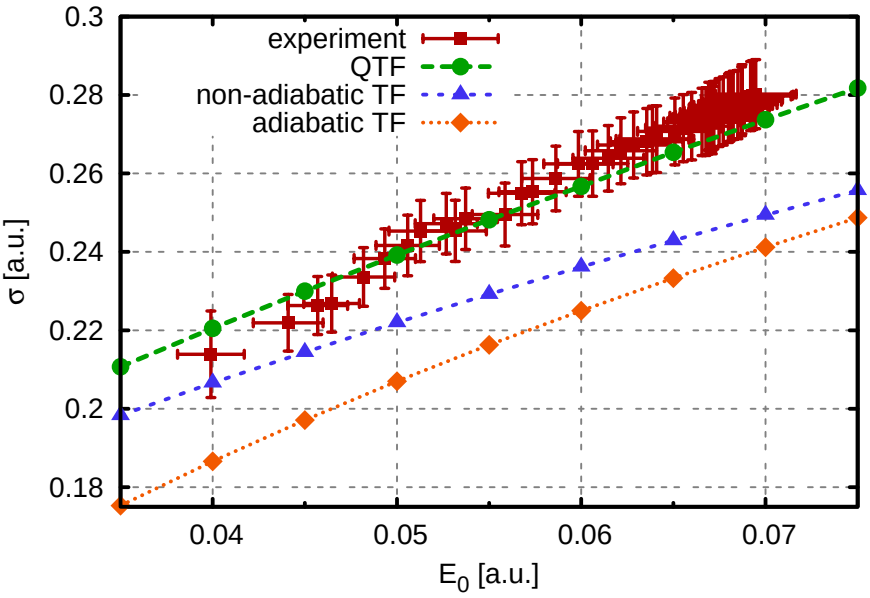

Figure 3: Width σ of the momentum distribution after strong-field ionization of the argon atom by an 800 nm field. Shown are experimental values from [12] (red squares), results from the QTF, Eq. (11), with a hydrogen-like $3p_z$ orbital (green circles), and the adiabatic (orange diamonds) and non-adiabatic (blue triangles) forms of the tunneling formula (TF), Eqs. (1) and (14).

to study the details of strong-field ionization. On the theory side, it remains to be investigated whether the remaining deviations for neon are due to the bound-state momentum distributions or due to multielectron effects.

Acknowledgements

We thank C. Smeenk for making the experimental data published in [12] available to us. Also we thank C. C. Chirilă for helpful discussions. We gratefully acknowledge support by the Deutsche Forschungsgemeinschaft that is funding the Centre for Quantum Engineering and Space-Time Research (QUEST).

[1] G. Steinmeyer, D. H. Sutter, L. Gallmann, N. Matuschek, U. Keller, Science 286 (1999) 1507.

[2] G. Sansone, E. Benedetti, F. Calegari, C. Vozzi, L. Avaldi, R. Flammini, L. Pletto, P. Villoresi, C. Altucci, R. Velotta, S. Stagira, S. D. Silvestri, M. Nisoli, Science 314 (2006) 443.

[3] Z. Chang, A. Rundquist, H. Wang, M. M. Murnane, H. C. Kapteyn, Phys. Rev. Lett. 79 (1997) 2967.

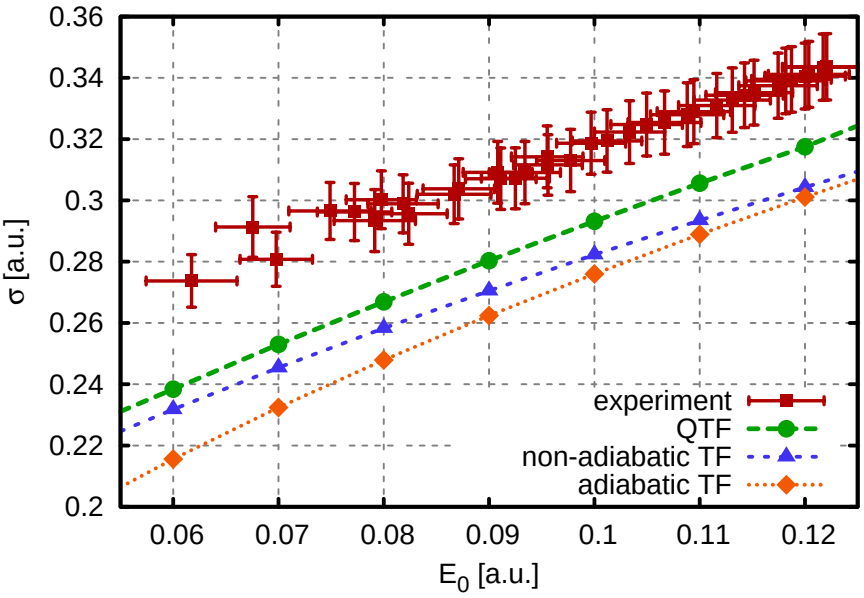

Figure 4: Width σ of the momentum distribution after strong-field ionization of the neon atom by an 800 nm field. Shown are experimental values from [12] (red squares), results from the QTF, Eq. (11), with a hydrogen-like $2p_z$ orbital (green circles), and the adiabatic (orange diamonds) and non-adiabatic (blue triangles) forms of the tunneling formula (TF), Eqs. (1) and (14).

[4] S. Haessler, J. Caillat, W. Boutu, C. Giovanetti-Teixeira, T. Ruchon, T. Auguste, Z. Diveki, P. Breger, A. Maquet, B. Carre, R. Taïeb, P. Salières, Nature Physics 6 (2010) 200.

[5] M. Drescher, M. Hentschel, R. Kienberger, M. Uiberacker, V. Yakovlev, A. Scrinzi, T. Westerwalbesloh, U. Kleineberg, U. Heinzmann, F. Krausz, Nature 419 (2002) 803.

[6] M. Uiberacker, T. Uphues, M. Schultze, A. J. Verhoef, V. Yakovlev, M. F. Kling, J. Rauschenberger, N. M. Kabachnik, H. Schröder, M. Lezius, K. L. Kompa, H.-G. Muller, M. J. J. Vrakking, S. Hendel, U. Kleineberg, U. Heinzmann, M. Drescher, F. Krausz, Nature 446 (2007) 627.

[7] S. Baker, J. S. Robinson, C. A. Haworth, H. Teng, R. A. Smith, C. C. Chirila, M. Lein, J. W. G. Tisch, J. P. Marangos, Science 312 (2006) 424.

[8] P. B. Corkum, F. Krausz, Nature Physics 3 (2007) 381.

[9] P. Dietrich, F. Krausz, P. B. Corkum, Opt. Lett. 25 (2000) 16–18.

[10] P. Eckle, M. Smolarski, P. Schlup, J. Biegert, A. Staudte, M. Schoffler, H. G. Muller, R. Dorner, U. Keller, Nat. Phys. 4 (2008) 565–570.

[11] P. Eckle, A. N. Pfeiffer, C. Cirelli, A. Staudte, R. Dörner, H. G. Muller, M. Büttiker, U. Keller, Science 322 (2008) 1525 –1529.

[12] L. Arissian, C. Smeenk, F. Turner, C. Trallero, A. V. Sokolov, D. M. Villeneuve, A. Staudte, P. B. Corkum, Phys. Rev. Lett. 105 (2010) 133002.

[13] R. Moshammer, B. Feuerstein, W. Schmitt, A. Dorn, C. D. Schröter, J. Ullrich, Phys. Rev. Lett. 84 (2000) 447.

[14] A. Rudenko, K. Zrost, T. Ergler, A. B. Voitkiv, B. Najjari, V. L. B. d. Jesus, B. Feuerstein, C. D. Schröter, R. Moshammer, J. Ullrich, J. Phys. B: At. Mol. Opt. Phys. 38 (2005) L191–L198.

[15] N. B. Delone, V. P. Krainov, J. Opt. Soc. Am B 8 (1991) 1207–1211.

[16] M. Y. Ivanov, M. Spanner, O. Smirnova, J. Mod. Opt. 52 (2005) 165.

[17] C. Smeenk, J. Z. Salvail, L. Arissian, P. B. Corkum, C. T. Hebeisen, A. Staudte, Opt. Express 19 (2011) 9336–9344.

[18] A. S. Alnaser, X. M. Tong, T. Osipov, S. Voss, C. M. Maharjan, B. Shan, Z. Chang, C. L. Cocke, Phys. Rev. A 70 (2004) 023413.

[19] J. Henkel, M. Lein, V. Engel, I. Dreissigacker (2011) submitted.

[20] M. Spanner, O. Smirnova, P. B. Corkum, M. Y. Ivanov, J. Phys. B: At. Mol. Opt. Phys. 37 (2004) L243–L250.

[21] D. I. Bondar, Phys. Rev. A 78 (2008) 015405.

[22] H. R. Reiss, Phys. Rev. A 22 (1980) 1786.

[23] F. H. M. Faisal, J. Phys. B 6 (1973) L89.

[24] L. V. Keldysh, Sov. Phys. JETP 20 (1965) 1307.

[25] B. Podolsky, L. Pauling, Phys. Rev. 34 (1929) 109.

[26] G. F. Gribakin, M. Y. Kuchiev, Phys. Rev. A 55 (1997) 3760.

[27] E. Clementi, D. L. Raimondi, J. Chem. Phys. 38 (1963) 2686.

[28] H. G. Muller, Phys. Rev. A 60 (1999) 1341.

[29] H. J. Wörner, H. Niikura, J. B. Bertrand, P. B. Corkum, D. M. Villeneuve, Phys. Rev. Lett. 102 (2009) 103901.

[30] X. M. Tong, C. D. Lin, J. Phys. B: At. Mol. Opt. Phys. 38 (2005) 2593.